Gravitational wave radiation from early universe turbulence

Spanish-Portuguese Relativity Meeting EREP 2021
Sep. 13–16, 2021

APC, CNRS, FRANCE

Alberto Roper Pol
Postdoctoral Researcher

Laboratoire Astroparticule et Cosmologie (APC)
Université de Paris, CNRS

Collaborators: A. Brandenburg (Nordita), C. Caprini (APC), G. Gogoberidze (Ilia State U), T. Kahniashvili (CMU), A. Kosowsky (PittU), S. Mandal (SBU), A. Neronov (APC), D. Semikoz (APC).

ARP *et al., Geophys. Astrophys. Fluid Dyn.* **114**, 130 (2020), arXiv:1807.05479
ARP *et al., Phys. Rev. D* **102**, 083512 (2020), arXiv:1903.08585
A. Neronov, ARP, C. Caprini, D. Semikoz., *Phys. Rev. D* **103**, L041302, arXiv:2009.14174 (2021)
T. Kahniashvili *et al., Phys. Rev. Res.* **3**, 013193 (2021), arXiv:2011.0556
ARP *et al.*, arXiv:2107.05356 (2021).

Overview

1. Introduction and Motivation
2. Primordial magnetic fields
3. Magnetohydrodynamics
4. Gravitational waves
5. Numerical Simulations

Introduction and Motivation

- Gravitational waves are opening a new window into our understanding of the Universe
  - First event GW150914 detected[1]

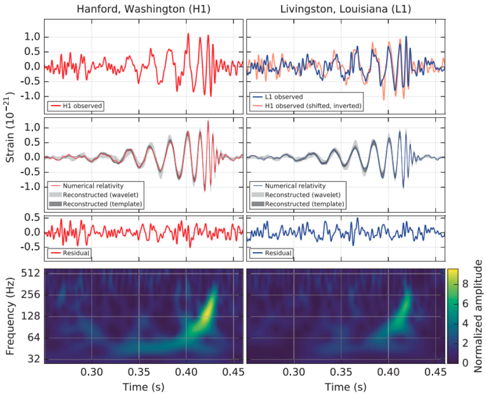

[1] [LIGO-Virgo Collaboration], *Phys. Rev. Lett.* **116**, 061102 (2016)

Introduction and Motivation

- GW170817 NS binary merger: first detection of GW and EM counterpart (constrain on the GW speed, measure of the Hubble factor)
- Several following events: LIGO-Virgo is currently on the second half of its third run of data (O3b) → 50 events up to O3a[2]

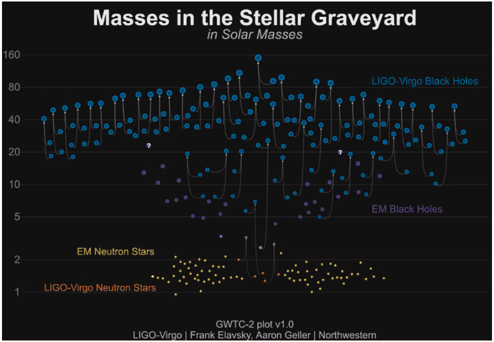

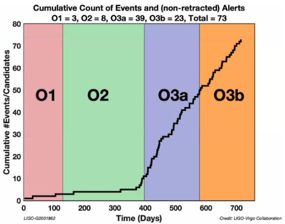

[2] [LIGO-Virgo Collaboration], GWTC-2, arXiv:2010.14527 (2020).

Introduction and Motivation

- Not only astrophysical, potential for cosmology sources
- Generation of cosmological GWs during phase transitions
  - LIGO-Virgo frequencies are 10–1000 Hz ($T \sim 10^7$ GeV)

    Peccei-Quinn, B-L, left-right symmetries, ...
    (untested physics, SM extensions)
  - **LISA** frequencies are 10^{-5}–10^{-2} Hz

    Electroweak phase transition ~ 100 GeV ($f_c \sim 10^{-5}$ Hz)
  - Pulsar Timing Array **(PTA)** frequencies are 10^{-9}–10^{-7} Hz

    Quantum chromodynamic (QCD) phase transition
    ~ 100 MeV ($f_c \sim 10^{-9}$ Hz)
- B-modes of CMB anisotropies ($f \sim 10^{-18}$ Hz)

  Inflation

Introduction and Motivation

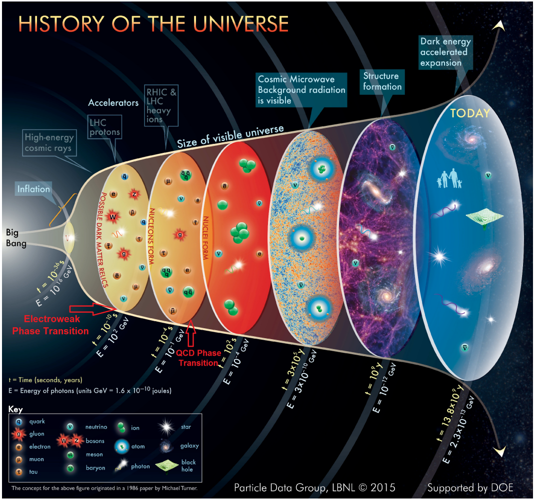

Gravitational Spectrum

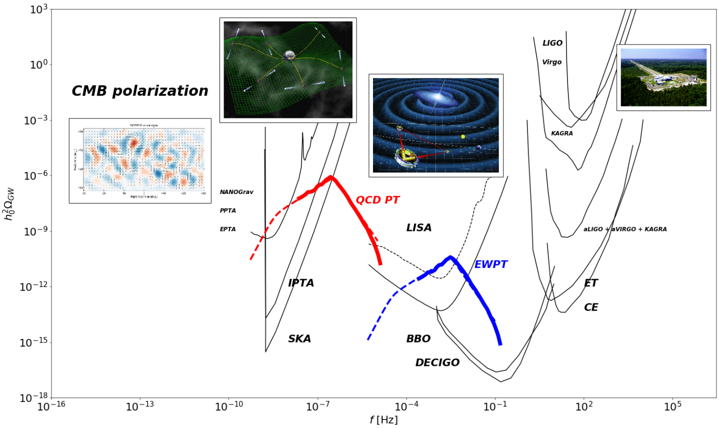

LISA

- Laser Interferometer Space Antenna (LISA) is a space–based GW detector
- LISA is planned for 2034
- LISA was approved in 2017 as one of the main research missions of ESA
- LISA is composed by three spacecrafts in a distance of 2.5M km
- LISA cosmology working group (since 2015, 230 members)

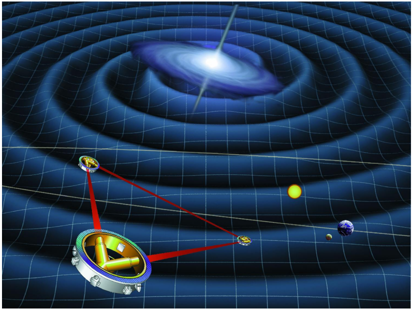

Figure: Artist's impression of LISA from Wikipedia

Introduction and Motivation

- Magnetohydrodynamic (MHD) sources of GWs
  - Hydrodynamic turbulence from first-order phase transitions
  - **Primordial magnetic fields**
- Other sources of GWs include
  - True vacuum bubble collisions
  - Sound waves
  - Cosmic topological defects (cosmic strings)
  - Primordial black holes

Introduction and Motivation

- Direct numerical simulations using the PENCIL CODE[3] to solve:
  - Relativistic MHD equations adapted for radiation-dominated era (after electroweak symmetry is broken)
  - Gravitational waves equation

[3] Pencil Code Collaboration, JOSS **6**, 2807 (2020), https://github.com/pencil-code/

Primordial magnetic fields

- Magnetic fields can either be produced at or present during cosmological phase transitions
- The magnetic fields are strongly coupled to the primordial plasma and inevitably lead to MHD turbulence[4]
- Present magnetic fields can be reinforced by primordial turbulence or generated via dynamo[5]
- Primordial magnetic fields would evolve through the history of the universe up to the present time and explain the lower bounds derived by the Fermi collaboration[6]
- Maximum amplitude of primordial magnetic fields is constrained by the big bang nucleosynthesis[7]

---

[4] J. Ahonen and K. Enqvist, *Phys. Lett. B* **382**, 40 (1996).

[5] A. Brandenburg, T. Kahniashvili, S. Mandal, A. Roper Pol, A. G. Tevzadze and T. Vachaspati *Phys. Rev. Fluids* **4**, 024608 (2019).

[6] A. Neronov and I. Vovk, *Science* **328**, 73 (2010)

[7] V. F. Shvartsman, Pisma Zh. Eksp. Teor. Fiz. 9, 315 (1969).

Evolution of magnetic strength and correlation length[8]

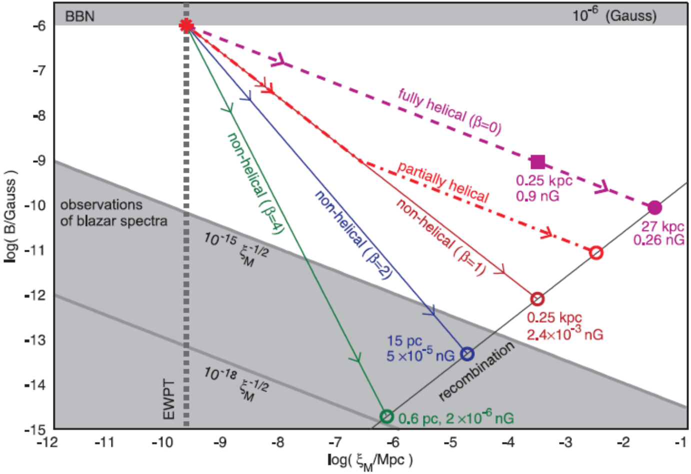

[8] A. Brandenburg, T. Kahniashvili, S. Mandal, A. Roper Pol, A. Tevzadze and T. Vachaspati, *Phys. Rev. D* **96**, 123528 (2017)

MHD description

Right after the electroweak phase transition we can model the plasma using continuum MHD

- Quark-gluon plasma (above QCD phase transition)
- Charge-neutral, electrically conducting fluid
- Relativistic magnetohydrodynamic (MHD) equations
- Ultrarelativistic equation of state

$$p = \rho c^2/3$$

- Friedmann–Lemaître–Robertson–Walker model

$$g_{\mu\nu} = \mathrm{diag}\{-1, a^2, a^2, a^2\}$$

Contributions to the stress-energy tensor

$$T^{\mu\nu} = \left(p/c^2 + \rho\right) U^\mu U^\nu + p g^{\mu\nu} + F^{\mu\gamma} F^{\nu}{}_{\gamma} - \frac{1}{4} g^{\mu\nu} F_{\lambda\gamma} F^{\lambda\gamma},$$

- From fluid motions
  $T_{ij} = \left(p/c^2 + \rho\right) \gamma^2 u_i u_j + p\delta_{ij}$
  Relativistic equation of state: $p = \rho c^2/3$
- From magnetic fields:
  $T_{ij} = -B_i B_j + \delta_{ij} B^2/2$

- 4–velocity $U^\mu = \gamma(c, u^i)$
- 4–potential $A^\mu = (\phi/c, A^i)$
- 4–current $J^\mu = (c\rho_{\mathrm{e}}, J^i)$
- Faraday tensor
  $F^{\mu\nu} = \partial^\mu A^\nu - \partial^\nu A^\mu$

Conservation laws

$$T^{\mu\nu}{}_{;\nu} = 0$$

Relativistic MHD equations are reduced to[9]

$$\frac{\partial \ln \rho}{\partial t} = -\frac{4}{3}\left(\boldsymbol{\nabla}\cdot\boldsymbol{u} + \boldsymbol{u}\cdot\boldsymbol{\nabla}\ln\rho\right) + \frac{1}{\rho}\left[\boldsymbol{u}\cdot(\boldsymbol{J}\times\boldsymbol{B}) + \eta\boldsymbol{J}^2\right],$$

$$\frac{D\boldsymbol{u}}{Dt} = \frac{1}{3}\mathrm{u}\left(\boldsymbol{\nabla}\cdot\boldsymbol{u} + \boldsymbol{u}\cdot\boldsymbol{\nabla}\ln\rho\right) - \frac{\boldsymbol{u}}{\rho}\left[\boldsymbol{u}\cdot(\boldsymbol{J}\times\boldsymbol{B}) + \eta J^2\right]$$

$$-\frac{1}{4}\boldsymbol{\nabla}\ln\rho + \frac{3}{4\rho}\boldsymbol{J}\times\boldsymbol{B} + \frac{2}{\rho}\boldsymbol{\nabla}\cdot(\rho\nu\boldsymbol{S}) + \mathcal{F},$$

$$\frac{\partial \boldsymbol{B}}{\partial t} = \boldsymbol{\nabla}\times\left(\boldsymbol{u}\times\boldsymbol{B} - \eta\boldsymbol{J} + \mathcal{E}\right),$$

for a flat expanding universe with comoving and normalized $p = a^4 p_{\mathrm{phys}}, \rho = a^4 \rho_{\mathrm{phys}}, B_i = a^2 B_{i,_{\mathrm{phys}}}, u_i$, and conformal time t.

---

[9] A. Brandenburg, *et al.*, *Phys. Rev. D* **54**, 1291 (1996)

GWs equation for an expanding flat Universe

- Assumptions: isotropic and homogeneous Universe
- Friedmann–Lemaître–Robertson–Walker (FLRW) metric $\gamma_{ij} = a^2\delta_{ij}$
- Tensor-mode perturbations above the FLRW model:

$$g_{ij} = a^2 \left(\delta_{ij} + h_{ij}^{\mathrm{phys}}\right)$$

- GWs equation is[10]

$$\left(\partial_t^2 - \cancel{\frac{a''}{a}} - c^2\nabla^2\right) h_{ij} = \frac{16\pi G}{a c^2} T_{ij}^{\mathrm{TT}}$$

  - h_{ij} are rescaled $h_{ij} = a h_{ij}^{\mathrm{phys}}$
  - Comoving spatial coordinates $\nabla = a\nabla^{\mathrm{phys}}$
  - Conformal time $\mathrm{d}t = a\,\mathrm{d}t^{\mathrm{phys}}$
  - Comoving stress-energy tensor components $T_{ij} = a^4 T_{ij}^{\mathrm{phys}}$
  - Radiation-dominated epoch such that $a'' = 0$

[10] L. P. Grishchuk, *Sov. Phys. JETP* **40**, 409 (1974).

Normalized GW equation[11]

$$\left(\partial_t^2 - \nabla^2\right) h_{ij} = 6\, T_{ij}^{\mathrm{TT}} / t$$

Properties

- All variables are normalized and non-dimensional
- Conformal time is normalized with t_*
- Comoving coordinates are normalized with c/H_*
- Stress-energy tensor is normalized with $\mathcal{E}_{\mathrm{rad}}^* = 3H_*^2 c^2/(8\pi G)$
- Scale factor is $a_* = 1$, such that $a = t$

[11] A. Roper Pol *et al.*, *Geophys. Astrophys. Fluid Dyn.* **114**, 130 (2020). arXiv:1807.05479.

Numerical results for decaying MHD turbulence[12]

Initial conditions

- Initial stochastic magnetic field with fractional helicity $\mathcal{P}_{\rm M} = 2\sigma/(1+\sigma^2)$
- Batchelor spectrum, i.e., $E_{\rm M} \propto k^4$ for small k
- Kolmogorov spectrum in the inertial range, i.e., $E_{\rm M} \propto k^{-5/3}$

$$kB_i = \left(P_{ij} - i\sigma\varepsilon_{ijl}\ \hat{k}_l\right) g_j \sqrt{2E_{\rm M}(k)},$$

$$E_{\rm M}(k) = \tfrac{1}{2} B_0^2 k_*^{-1/2} \frac{(k/k_*)^4}{\left(1+(k/k_*)^{34/3}\right)^{1/2}}$$

[12] A. Brandenburg *et al.* *Phys. Rev. D* **96**, 123528 (2017)
A. Roper Pol *et al.* *Phys. Rev. D* **102**, 083512 (2020)
A. Roper Pol *et al.* arXiv:2107.05356

Numerical results for decaying MHD turbulence

Initial conditions

- Magnetic energy density at t_* is a fraction of the radiation energy density, $\mathcal{E}_\mathrm{M}/\mathcal{E}^*_\mathrm{rad} = \frac{1}{2}B_0^2 \leq 0.1$ (BBN limit).
- Spectral peak $k_* = N_* \times 2\pi$, normalized by H_*/c is given by the characteristic scale of the sourcing turbulence (as a fraction of the Hubble radius).

Numerical results for decaying MHD turbulence for $N_* = 100, \mathcal{E}_\mathrm{M} \sim 10^{-2}$

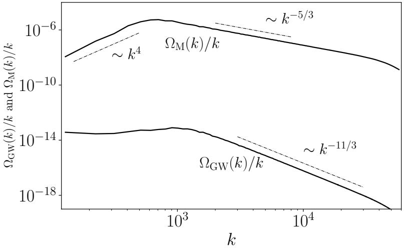

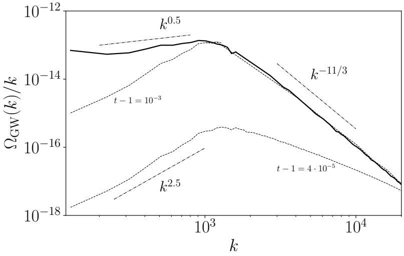

- **Novel k^0 scaling in the subinertial range, i.e., $\Omega_\mathrm{GW}(f) \sim f$**
- k^2 is expected for larger scales, i.e., $\Omega_\mathrm{GW}(f) \sim f^3$
- Further investigation on the k^0 development

Detectability of the SGWB from the EWPT with LISA (for decaying MHD turbulence with initial magnetic field)[13]

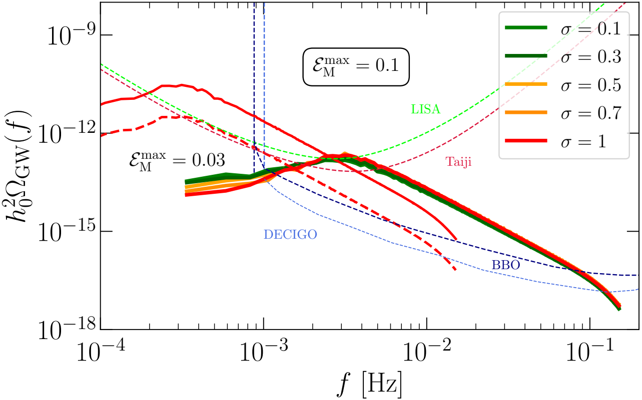

[13] A. Roper Pol, *et al.* *Phys. Rev. D* **102**, 083512 (2020)

A. Roper Pol, *et al.* arXiv:2107.05356

Numerical results for decaying MHD turbulence[14]

Driven magnetic field

- Initial magnetic and velocity are zero
- Magnetic field is built-up for a short duration ($\sim 0.1 H_*^{-1}$) via the induction equation

$$\frac{\partial \boldsymbol{B}}{\partial t} = \boldsymbol{\nabla} \times \left(\boldsymbol{u} \times \boldsymbol{B} - \eta \boldsymbol{J} + \mathcal{F} \right).$$

- The forcing term is quasi-monochromatic with fractional magnetic helicity

$$\mathcal{F} \; = \mathrm{Re}(\mathcal{A} \boldsymbol{f}) \exp\left[i \boldsymbol{k} \cdot \boldsymbol{x} + i\phi \right], \quad k_* - \tfrac{1}{2}\delta k \leq |\boldsymbol{k}| \; \leq k_* + \tfrac{1}{2}\delta k$$

$$f_i = \left(\delta_{ij} - i\sigma \varepsilon_{ijl} \hat{k}_l \right) f_j^{(0)} / \sqrt{1 + \sigma^2}$$

[14] A. Roper Pol, *et al.* *Phys. Rev. D* **102**, 083512 (2020)
A. Roper Pol, *et al.* arXiv:2107.05356

Detectability of the SGWB from the EWPT with LISA (for decaying MHD turbulence with an initially forced magnetic field)[15]

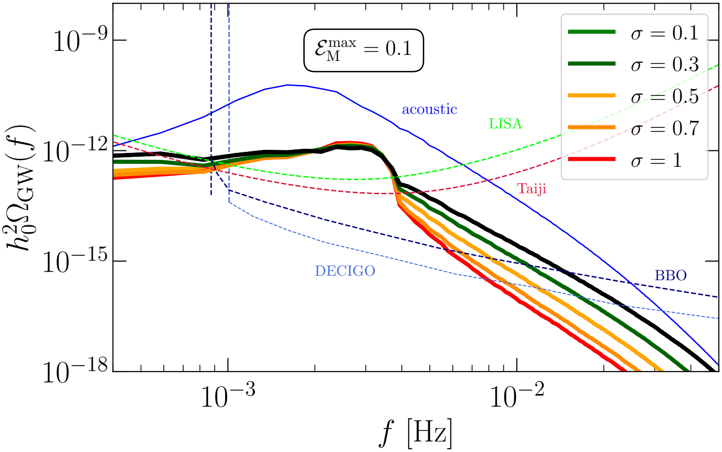

[15] A. Roper Pol *et al.* *Phys. Rev. D* **102**, 083512 (2020)
A. Roper Pol *et al.* arXiv:2107.05356

Polarization degree from stationary turbulence (long-time forcing)

- Helical magnetic fields induce circularly polarized GWs[16]

- Kinetic turbulence

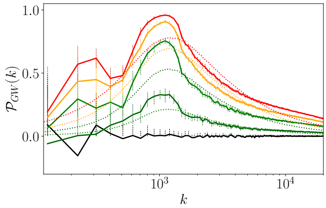

- Magnetic turbulence

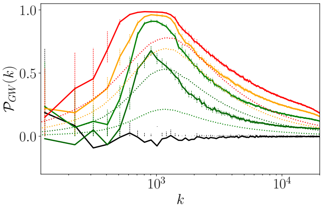

- Degree of circular polarization

$$\mathcal{P}_{\rm GW}(k) = \frac{\Xi_{\rm GW}(k)}{\Omega_{\rm GW}(k)} = \frac{\left\langle \dot{\tilde{h}}_\times \dot{\tilde{h}}_+^* - \dot{\tilde{h}}_+ \dot{\tilde{h}}_\times^* \right\rangle}{\left\langle \dot{\tilde{h}}_+ \dot{\tilde{h}}_+^* + \dot{\tilde{h}}_\times \dot{\tilde{h}}_\times^* \right\rangle}$$

[16] L. Kisslinger and T. Kahniashvili, Phys. Rev. D **92**, (2015)
T. Kahniashvili, G. Gogoberidze and B. Ratra, Phys. Rev. Lett. **95**, 151301 (2005)
T. Kahniashvili, A. Brandenburg, A. Kosowsky, S. Mandal, A. Roper Pol, *Phys. Rev. Res.* **3**, 013193 (2021)

Detectability of the polarized SGWB from the EWPT with LISA and Taiji[19]

- LISA's dipole response function can provide us with a polarized gravitational wave background due to our proper motion[17]
- Cross-correlation of LISA and an additional space-based GW detector can improve the detectability of a polarized GW background[18]

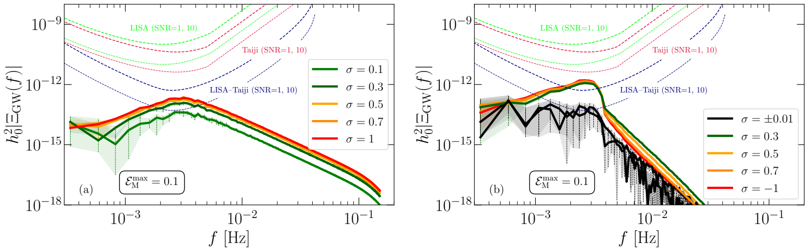

[17] V. Domcke, et al., JCAP **05**, 028 (2020)

[18] G. Orlando, M. Pieroni and A. Ricciardone, JCAP **03**, 069 (2021)

[19] A. Roper Pol *et al.* arXiv:2107.05356

NANOGrav 12.5 yr data observation[20]

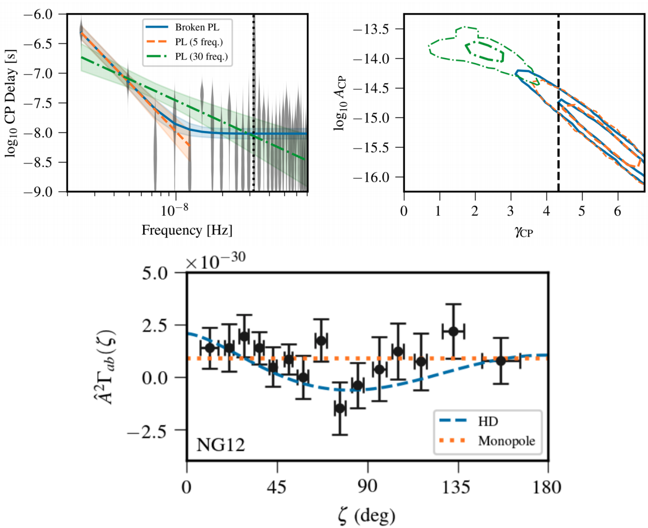

---

[20] NANOGrav collaboration, ApJ Lett., **905**, 2 (2020)

Detectability of the SGWB produced by non-helical primordial magnetic fields from the QCD phase transition by NANOGrav[21]

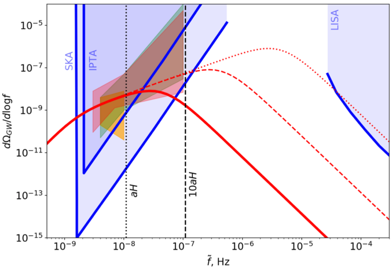

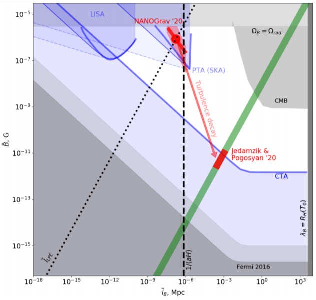

21 A. Neronov, A. Roper Pol, C. Caprini, D. Semikoz, *Phys. Rev. D* 103, L041302 (2021)

Conclusions 1/2

- Depending on the mechanism of turbulence generation and/or the initial energy density and characteristic scale, the GW signal from the EWPT is detectable by LISA.
- General f spectrum obtained for GWs in the low frequency range vs f^3 obtained from analytical estimates (below horizon scales).
- Bubble nucleation and magnetogenesis physics can be coupled to our equations for more realistic production analysis
- Detection of GW spectrum can provide *clean* information from the epoch of generation and the turbulence characteristics.
- The circular polarization of GWs produced by helical magnetic fields can be detected by LISA and improved by correlating LISA and additional space-based GW detectors (e.g., TianQin, Taiji)
- Polarization degree can provide information on magnetic helicity of the seed field, about its nature (kinetically or magnetically dominant), and formation process.
- Potential detection by NANOGrav if magnetic scale is near horizon.

Conclusions 2/2

- A lot of interesting science has been and can be done in a very unique time for GW astronomy with future GW detectors (LISA, IPTA, SKA, CE, ET, BBO, DECIGO, atomic interferometry, Gaia, CMB anisotropies with LiteBIRD, ...)
- Production of helical magnetic fields can be related to Chern-Simons violations and to production of particles, shedding light into the baryon-asymmetry problem
- Probe of the origin of magnetic fields in the largest scales of our Universe, which is still an open question in cosmology

The End

Thank You!

APC, CNRS, FRANCE

Laboratory for Atmospheric and Space Physics
University of Colorado **Boulder**

NORDITA
The Nordic Institute for Theoretical Physics

SHOTA RUSTAVELI NATIONAL SCIENCE FOUNDATION

roperpol@apc.in2p3.fr